Superhydrophobic polydimethylsiloxane dip-coated polycaprolactone electrospun membrane for extracorporeal membrane oxygenation

Zhuomin Jiang, Bao Tran Duy Nguyen, JeongHyeon Seo, Changgi Hong, Dongwoo Kim, Suhyun Ryu, Sohui Lee, Gyubok Lee, Young Hoon Cho, Jeong F. Kim, Kangwon Lee

PII: S0376-7388(23)00371-X

DOI: https://doi.org/10.1016/j.memsci.2023.121715

Reference: MEMSCI 121715

To appear in: *Journal of Membrane Science*

Received Date: 10 January 2023

Revised Date: 25 April 2023

Accepted Date: 1 May 2023

Please cite this article as: Z. Jiang, B.T.D. Nguyen, J. Seo, C. Hong, D. Kim, S. Ryu, S. Lee, G. Lee, Y.H. Cho, J.F. Kim, K. Lee, Superhydrophobic polydimethylsiloxane dip-coated polycaprolactone electrospun membrane for extracorporeal membrane oxygenation, *Journal of Membrane Science* (2023), doi: https://doi.org/10.1016/j.memsci.2023.121715.

Graphical Abstract

Superhydrophobic polydimethylsiloxane dip-coated polycaprolactone electrospun membrane for extracorporeal membrane oxygenation

Zhuomin Jiang, Bao Tran Duy Nguyen, JeongHyeon Seo, Changgi Hong, Dongwoo Kim, Suhyun Ryu, Sohui Lee, Gyubok Lee, Young Hoon Cho*, Jeong F. Kim*, Kangwon Lee**

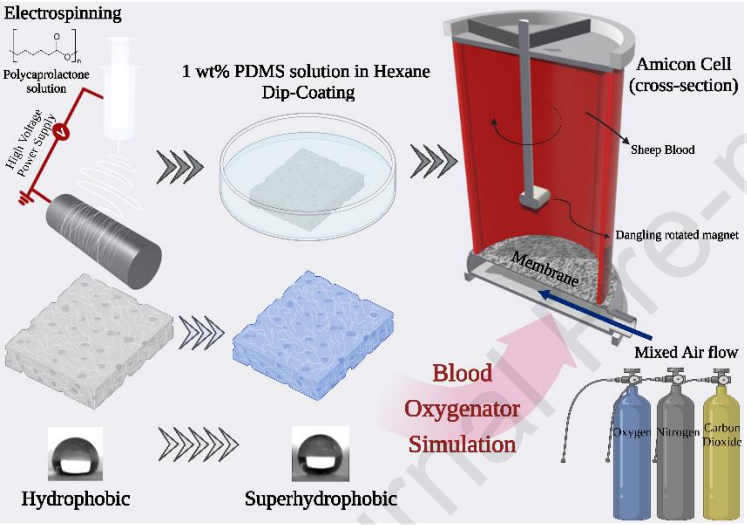

Figure was created using BioRender (agreement number: YZ259I72A8).

Superhydrophobic polydimethylsiloxane dip-coated polycaprolactone electrospun membrane for extracorporeal membrane oxygenation

Zhuomin Jiang[a,b], Bao Tran Duy Nguyen[c], JeongHyeon Seo[d], Changgi Hong[a,b], Dongwoo Kim[a,b], Suhyun Ryu[a,b], Sohui Lee[a,b], Gyubok Lee[a,b], Young Hoon Cho*[d,e], Jeong F. Kim*[c,f], Kangwon Lee**[a,b]

[a] *Department of Applied Bioengineering, Graduate School of Convergence Science andTechnology, Seoul National University, Seoul, 08826, Republic of Korea*

[b] *Research Institute for Convergence Science, Seoul NationalUniversity, Suwon-si, Gyeonggi-do, Republic of Korea*

[c] *Department of Energy and Chemical Engineering, Incheon NationalUniversity, Incheon, Republic of Korea*

[d] *Green Carbon Research Center, Chemical and Process Technology Division, KoreaResearch Institute of Chemical Technology, Daejeon, 34114, Republic of Korea*

[e] *Advanced Materials and Chemical Engineering, University of Science and Technology, Daejeon, 34113, Republic of Korea*

[f] *Innovation Center for Chemical Engineering, Incheon National University, Incheon, Republic of Korea*

* Corresponding author **Dr. Young Hoon Cho**. Green Carbon Research Center, Chemical & Process Technology Division, Korea Institute of Chemical Technology (KRICT), 141 Gajeong-ro, Yuseong-gu, Daejeon, 34114, Republic of Korea.

* Corresponding author **Prof. Jeong F. Kim**. Department of Energy and Chemical Engineering, Incheon National University, Incheon, Republic of Korea.

** Corresponding author **Prof. Kangwon Lee**. Department of Applied Bioengineering, Graduate School of Convergence Science andTechnology, Seoul National University, Seoul, 08826, Republic of Korea.

Email Address: Prof. Kangwon Lee: kangwonlee@snu.ac.kr; Prof. Jeong F. Kim: JeongKim@inu.ac.kr; Dr. Young Hoon Cho: yhcho@krict.re.kr

Abstract

Extracorporeal membrane oxygenation (ECMO) is a technique that delivers gas exchange to cardiopulmonary surgery patients. Membrane oxygenation failure may result in serious health problems for patients due to ECMO membrane wetting and surface fouling problems. Thus, in this work, the superhydrophobic membrane is designed to improve the resistance to wetting and long-term fouling of the ECMO membrane. The hydrophobic biocompatible polycaprolactone (PCL) was used to fabricate an electrospun nanofiber membrane. Polydimethylsiloxane (PDMS) was dip-coated on the PCL electrospun membrane to enhance the membrane hydrophobicity, which lifts the water contact angle from 136 to 160 degrees. The PDMS90 membrane shows low protein adsorption under 10 *m*g/*m*L BSA incubation, inhibiting the platelet activation and intensifying long-term antifouling of the membrane. The lab-scale blood oxygenation results indicate that the developed membrane is competitive with the commercial polypropylene (PP) and lab-made polymethyl pentene (PMP) membranes. In conclusion, the conducted experiments verify that the developed membrane has the potential to be applied to the ECMO membrane.

Keywords: artificial lung, blood oxygenation membrane, ECMO membrane, superhydrophobic membrane, poly(ϵ-caprolactone) (PCL), polydimethylsiloxane (PDMS)

1. Introduction

With the advent of Coronavirus disease (COVID-19) [1][2], researchers have attracted attention to Cardiopulmonary bypass (CPB) [3], also named as Artificial lung (AL). Extracorporeal membrane oxygenation (ECMO) has developed together with such interest. ECMO plays a crucial role in providing respiration assistance to severe respiratory patients by assisting the gas exchange from outside of the body during heart surgery. The oxygenator is the main component of the ECMO machine. Membrane oxygenators are used to oxygenate blood by indirect contact between venous blood and oxygen, and the differential partial pressure exchanges oxygen and carbon dioxide [4].

In recent years, the ECMO market has been driven by dense poly-4-methyl pentene (PMP) and porous polypropylene (PP) membranes [5]. ECMO membrane is divided into dense membranes and porous membranes. Dense membranes provide gas exchange by material intrinsic gas

solubility and diffusivity [6]. Porous membranes, on the other hand, deliver gas through the pores in the membrane. Hence, the pore distribution and aperture size affect the porous membrane oxygenation capacity [7] and lifespan [8]. Several existing methods for producing ECMO membrane substrate are phase inversion [9][10], 3D printing [11], and spin coating with initiated chemical vapor deposition [12]. Meanwhile, electrospinning can produce a porous membrane, and the fiber diameter and the number of layers may affect the membrane pore size [13][13][15][16][17]. Therefore, electrospun membrane with smaller fiber diameter and denser layers has a potential to be exploited in the gas exchange of ECMO membranes.

Although the hydrophobic porous membrane has better blood oxygenation efficiency, blood tends to coagulate in the pores by capillary effect and leads to a serious plasma leakage to the membrane. Once the membrane is wet, the oxygenation efficiency decreases and potentially endangers the patient's life. For this concern, the membrane substrate must be hydrophobic to avoid wetting and prevent plasma leakage during blood oxygenation. However, an ECMO machine requires a large surface area of the blood-contacting membrane for adequate gas exchange, which brings concern to membrane hemocompatibility [18]. As the hydrophobic surface is susceptible to protein foulants and the hydrophobic interactions act with the blood components (such as protein, platelet, and cells) [19][19][20], the hazardous compounds might release and activate the blood immune system after the membrane directly contacts the blood [22]. Thus, the long-term operation challenges of membrane oxygenators are hemocompatibility and antifouling properties [5].

Antifouling studies mainly aim to reduce the formation of thrombosis by inhibiting the activation and aggregation of the platelet. Since the leading causes of thrombosis are protein adsorption and cell adhesion on the surface [23][24], hydrophilic [25] and superhydrophobic modifications [26] are employed to improve the surface hemocompatibility and subsequently elevate the surface antifouling property.

The utilization of hydrophilic coating layers is the common surface modification method that can inhibit blood clotting. Nitric oxide (NO) [26] and heparin [28] coating layers have been demonstrated to suppress blood coagulation cascades, and phosphorylcholine (PC) [29] coating has been found to reduce thrombosis. The poly (2-methoxyethyl acrylate) (PMEA) [30] covering has been proven to diminish platelet adherence. However, the long-term wetting of hydrophilic coating layers may limit ECMO performance and lifespan with unforeseen biofouling, particularly for porous membranes [31]. Hence, the hydrophilic coating layer might be difficult to balance between hemocompatibility and long-term antifouling.

To overcome membrane long-term fouling, superhydrophobic surface modifications have also been investigated for blood-contacting medical equipment and healthcare devices [32][33]. Membrane superhydrophobicity could be improved by reducing the effective area, which can also improve the surface hemocompatibility of the membrane [25]. The followings are the several methods to improve superhydrophobicity: nanoparticle coating [34], plasma treatment [35], chemical vapor deposition [36], vapor-induced phase separation [37], and electrospinning [38]. The reported superhydrophobic modification demonstrates impressive wetting resistance, protein fouling prevention, and antifouling in various gas-liquid contacting and biomedical membrane applications.

In this sense, polycaprolactone (PCL) can be a good option for producing ECMO membranes since it is a semi-crystalline hydrophobic polymer [39][40] with good hemocompatibility [41]. As an FDA- approved material [42], PCL has also been used in medical applications such as surgical sutures [43], blood vessel grafts [44][45], and tissue regeneration scaffolds [46]. However, hemocompatible PCL electrospun membrane is less durable and not strong enough to face long-term ECMO challenges, such as plasma leakage and antifouling. Accordingly, superhydrophobic modification, such as PDMS coating, is introduced to improve the PCL electrospun membrane property for the aforementioned ECMO challenges. PDMS, an FDA-approved hydrophobic polymer [47], is advantageous because it can provide superhydrophobicity to the membrane surface by simple modification [48][49][50][51].

In this work, a novel superhydrophobic ECMO membrane is created by PDMS dip-coating on a hydrophobic PCL electrospun membrane substrate to improve the hemocompatibility and gas transfer rate in long-term extracorporeal membrane oxygenation. The gradient PCL electrospun membrane was fabricated with different concentrations to provide a hydrophobic porous substrate. The PDMS solution is then diluted in hexane and dip-coated on the membrane surface throughout various periods. The hemocompatibility of PDMS-coated PCL electrospun membranes was characterized by hemolysis, blood clotting index, protein adsorption, cell cytotoxicity, platelet adhesion, and long-term antifouling tests. In addition, sheep blood was applied to simulate the blood oxygenation of the membranes. Figure 1 depicts the overall manufacturing process of the PDMS-coated PCL electrospun membrane and the oxygenation simulation of the membrane.

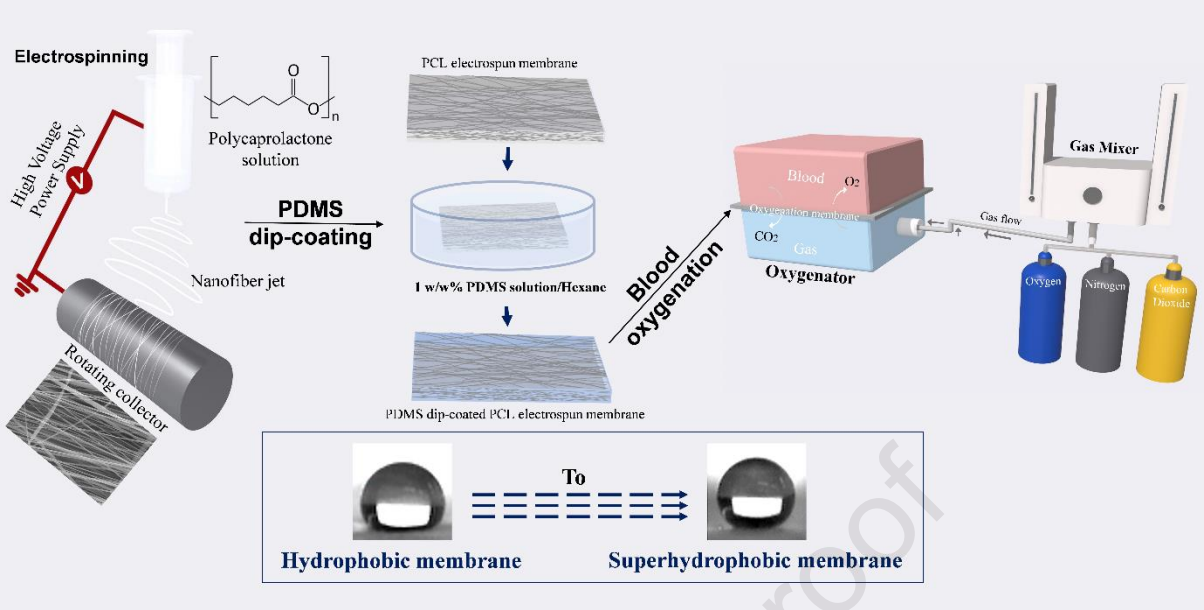

Figure 1. Schematic illustration of the preparation of the PDMS-coated PCL electrospun membrane for artificial oxygenation.

2. Experimental Section

2.1 Materials

Polycaprolactone (PCL) (Mw=80,000), Acetic acid (AA) (≥ 99%), N, N-Dimethylformamide (DMF) (99.8%), PP membrane, PMP raw material and bovine serum albumin (BSA) were purchased from Sigma Aldrich. Sylgard 184 A, B (PDMS prepolymer, curing agent) were purchased from Sewang Hitech Silicone. Chloroform (CF) (99.8%), Formic acid (FA) (99.0%), n-Hexane (96.0%) were purchased from Samchun pure chemical CO., LTD. Human umbilical vein endothelial cells (HUVECs) and culture medium (EBM-2 EGM-2 Bulletkit) were purchased from Lonza. Sheep blood defibrinated and citrated were purchased from KisanBio Inc.

2.2 Gradient nanofiber by electrospinning

Electrospun gradient PCL membrane were prepared with different solvents and weight ratios. The first finer layer was prepared by dissolving 9 wt% of PCL in Formic acid (FA)/ Acetic acid (AA) 7/3 (*v/v*) solution. The solution was mixed overnight at room temperature. Then the solution was electrospun for 10 hours into nanofibers at room temperature with a voltage of 17 *k*V, pump speed of 0.2 *m*L/*h*, and a 23 *cm* distance between the needle tip and the aluminum foil-covered rotating drum

collector. The second denser layer was prepared by dissolving 11 wt% PCL in Chloroform (CF)/ N, N-Dimethylformamide (DMF) 8/2 (*v/v*) solution. After overnight mixing, the solution was electrospun for 27 hours into nanofibers at room temperature with a voltage of 15 *k*V, pump speed of 1 *m*L/*h*, and a 23 *cm* distance between the needle tip and the aluminum foil-covered rotating drum collector. The third layer had the same experiment setting as the first layer. The final membrane was vacuum dried overnight to remove the residual solvents and to be ready for the later process.

2.3 Polydimethylsiloxane (PDMS) modification

Polydimethylsiloxane (PDMS)-modified PCL membranes were prepared by dip-coating method. 1 wt% (*w/w*) of PDMS solution (prepolymer: curing agent kit *w/w* 10: 1) was dissolved in n-hexane. The solution was light avoiding-stirred with a magnetic rod for 30min at room temperature. Then the PCL electrospun membranes were immersed in PDMS/n-hexane solution with varying periods (30 min, 60 min, 90 min) at room temperature. After that, the coated membranes were dried overnight in a vacuum oven at 40 ℃. The obtained membranes are denoted as PDMS30, PDMS60, PDMS90, respectively.

2.4 Characterization of membrane

Membrane morphologies and chemical compositions were characterized with FE-SEM and Silicon Drift Detector EDS (JSM-7800F Prime, JEOL Ltd, Japan) at 5 *k*V and 15 *k*V, respectively. A prior platinum layer was coated on the membrane surface before SEM scanning by Sputter Coater (Cressington 108 auto, Watford, UK). ATR-FTIR measurements were proceeded by TENSOR 27 (Bruker, Germany) ATR - FTIR spectrometer at 25 °C. Sample membranes were properly vacuum dried and direct measured under the spectra of 64 scans with a resolution of 2 cm^{-1}. Membrane surface roughness was investigated by Atomic Force Microscope (Park NX10, Park systems, Korea) over a scan area of 10 × 10 μm^2. The mechanical property of the membranes was conducted following the ASTM standard using a test window frame to hold the 1 × 4 cm^2 membrane. After loading the sample on the Universal Testing Machine (Instron 5543, Instron Corp, MA, USA), the vertical ribs were cut just before the start of the tensile test. Membrane tensile strength was tested with

a 100 *N* load cell and a 5 *mm*/*min* strain rate. The membrane surface contact angle of water, Ethylene Glycol and blood was measured by contact angle analyzer (Phoenix 300, SEO Co., Korea) with 2 μL of Deionized (DI) water and Ethylene Glycol, and 4 μL of citrated sheep blood (KisanBio Ltd., Seoul, South Korea). The average membrane pore size was examined by gas-liquid porometers (POROLUX™ 1000, Porometer Ltd, Belgium). The membrane liquid entry pressure (LEP) was determined after every 30 minutes from applying rising pressure to the membrane with 0.5 bar. The membrane was fixed under the water by Amicon ® cell for 24 hours before testing. The membrane was immersed in water for 24 hours before the LEP test. The LEP data was recorded at the first water drop fell. Membrane air permeance was investigated by the capillary flow porometer (model CFP-1500-AEL, Porous Materials Inc, NY, USA). The gas was supplied with 1 *bar* pressure to enter the membrane with a 1.8 *cm* diameter filter holder. Air permeance was denoted as gas permeation unit (GPU), where 1 GPU= $1\times10^{-6}\times(cm^3(\mathrm{STP})/cm^2\cdot cmHg\cdot sec)$. The thickness of membranes was measured by a digital micrometer (Coolant Proof IP65, Mitutoyo, USA).

2.5 Membrane Blood Oxygenation

The blood oxygenation test was measured using Amicon® Stirred Cells under 36 °C. All the membrane samples were punched into a circular-shaped membrane with a 4.25 *cm* diameter and installed in the Amicon® Stirred Cells for blood oxygenation tests. Defibrinated sheep blood (50 *m*L) was poured onto the top of the test membrane and stirred by a dangled magnetic rod at 200 *rpm* for deoxygenating blood and 400 *rpm* for the oxygenation test, respectively. The circulated gases flowed underneath the membrane by the tube connection between Amicon® Stirred Cells and the gas tanks. After loading the sterilized membrane on the cell, the deoxygenation process took 6 hours of nitrogen gas flowing at a 45 *cc*/*min* flow rate and carbon dioxide gas flowing at 4.5 *cc*/*min*. When the oxygen level was lower than 40 *mmHg* (measured by i-Smart 300 VET Blood Gas Analyser, i-SENS Inc., South Korea), oxygen gas was connected to the cell, and started the oxygenation test at a 50 *cc*/*min* flow rate. The membrane blood oxygenation property was simulated by the Amicon® cell (Figure S4). The dangling rotated magnet inside the Amicon® cell mixed the sheep blood to balance the sheep blood oxygen level inside the Amicon® cell for getting reliable data. The variations in blood oxygen level were recorded every 5 minutes until the oxygen level went beyond 200

mmHg. The CO_2/O_2 exchange rate calculation was based on the margins of blood oxygen over a settled period. The oxygen transfer rate (*m*L $O_2/m^2/min$) was calculated by dividing the total O_2 transfer quantity (*m*L O_2) by the blood-contacting area of the membrane (m^2). The total O_2 transfer quantity is the sum of total O_2 bound to hemoglobin (hbO_2) and dissolved O_2 in plasma (plO_2).

$$\textit{Oxygen transfer rate (mL } O_2/m^2/min) = \frac{d(sO_2+bO_2)}{dt \cdot A} \quad (1)$$

Where sO_2 is the oxygen dissolving volume (*m*L) in blood, bO_2 is the oxygen volume (*m*L) bound to hemoglobin, t is the time (*min*), and A is the tested membrane area (m^2).

2.6 Protein adsorption

The static membrane protein adsorption test was implemented with a petri dish. The 2×2 cm^2 membrane was first immersed in PBS and equilibrium under UV sterilization for 3 hours. After discarding the PBS, 2 *m*L of bovine serum albumin (BSA) (Sigma-Aldrich, USA) with 10 *m*g/*m*L concentration in PBS was prepared and submerged on the membrane surface, followed by incubating for 3/6/9 hours respectively at 37 ℃ with a 5% CO_2 incubator. After aspirating the BSA solution from the well, the membrane was rinsed gently with PBS three times to wash out non-absorbed protein. Then the membrane was immersed in 2 wt% aqueous sodium dodecyl sulfate (SDS) solution for 1 hour in the 37 ℃ incubator and 1 hour with a shaking table under room temperature to remove the adsorbed protein from the membrane. The membrane protein concentration and standard curve were measured by a BCA kit. In short, 25 μL of membrane solution and 200 μL of working reagent (A: B 50:1) were pipetted into a 96-well plate. After 30 seconds of gently plate shaking, the foil-covered 96-well plate was incubated in the 37 ℃ incubator for 2 hours. Lastly, the protein adsorption amount of the membrane was measured by the microplate reader (BioTek Synergy H1 Hybride Multi-mode reader, Agilent technologies, United States) with 562 *nm* absorbance.

2.7 Platelet adhesion

Firstly, citrated sheep blood (KisanBio Ltd., Seoul, South Korea) was centrifuged at 3500 *rpm* for 15 *min*, and the platelet rich plasma (PRP) suspension was extracted

and measured using the Countess II (Invitrogen) which showed 7×10^7 U/*m*L. UV sterilized 1×1 cm^2 membrane was placed in the petri dishes, and PBS solution was added to equilibrate membrane surface at room temperature for 2 hours and incubated for 30 min. After discarding the PBS solution, 100 μL PRP was added onto each side of the membrane surfaces and incubated in the 37 ℃ humidified incubator with 5% CO_2 flow for 2 hours. Then the sample was rinsed with PBS solution 3 times to remove the non-adherent platelets. The membrane was immersed into 2.5 wt% glutaraldehyde aqueous solution at 4 ℃ for 24 hours to immobilize the platelets on the sample surface. Subsequently, the membrane was rinsed three times by PBS and dehydrated by a graded ethanol (v/v) from PBS (0%, 10%, 25%, 50%, 75%, 100%) with 10 *min* for each step. Lastly, the platelets-adhered surface was observed by SEM.

2.8 Hemolysis rate

All the samples were cut into 1×1 cm^2 and immersed in 1.5 *m*L PBS and were incubated in the 37 ℃ humidified incubator with 5% CO_2 flow for 2 hours. After incubation, 30 μL of citrated sheep blood (KisanBio Ltd., Seoul, South Korea) were added into the microtube with further 2 hours of incubation. Afterward, the microtubes were centrifuged at 2500 rpm for 30 minutes. The supernatant was extracted into a 96-well plate with 200 μL per well and measured by a microplate reader (BioTek Synergy H1 Hybride Multimode reader, Agilent technologies, United States) under the 545 *nm*. The positive control was prepared by dissolving 30 μL of citrated sheep blood in 1.5 *m*L of deionized water, while the negative control was prepared by adding 30 μL of blood to a PBS solution. The calculation of hemolysis rate (HR) was calculated as follows:

$$HR = [(A_{sample} - A_{negative}) / (A_{positive} - A_{negative})] \times 100\% \quad (2)$$

2.9 Blood clotting index

The blood clotting test was operated with citrated sheep blood (KisanBio Ltd., Seoul, South Korea). The 5×5 mm^2 samples were immersed with deionized water within the 2 *m*L microtube for 1 hour incubation. After discarding the deionized water, 60 μL of blood and 4.5 μL of 0.2 M calcium chloride aqueous solution were pipetted

to contact the surface of the membrane and incubated for 5 min. Subsequently, 1.5 *m*L of deionized water was dropped into the microtube without directly touching the membrane surface. 200 μL of the supernatant was tested within a 96-well plate under the 540 *nm* by the microplate reader (BioTek Synergy H1 Hybride Multi-mode reader, Agilent technologies, United States). The negative control group was prepared by dissolving 60 μL of blood in 1.5 *m*L of the deionized water. The process has been repeated three times to collect the average data. The blood clotting index (BCI) was calculated by:

$$BCI\ (\%) = [(A_{sample})/(A_{negative})] \times 100\% \quad (3)$$

2.10 Cytotoxicity

Human Umbilical Vein Endothelial Cells (HUVEC) were selected to be the model cell to detect the membrane cytotoxicities (PCL, PDM90, PP, and PMP membranes) by direct contact Cell Counting Kit-8 (CCK-8) assay. The samples for CCK-8 cytotoxicity test were prepared with 5 × 5 mm^2. After 90 *min* of UV sterilization, the samples were equilibrated with PBS 3 times (1 hour/time). The HUVEC cells were pre-seeded into a 96-well plate with a density of 1×10^4 cells per well with overnight incubation. Before the input of membrane samples, the culture medium was replaced by the non-antibiotic fresh medium (EBM-2, Lonza). The sample-immersed plates were cultured at 37 ℃ with 5% CO_2 for 24 h, 48 h, and 72 h, respectively. The non-sample-immersion control was performed as a blank control for each time point. For each measurement, the samples and culture medium were carefully discarded, and 10% CCK-8 solution with fresh medium (110 μL) was pipetted into each well, followed by 45 *min* incubation. The absorbance results of each well were determined by the microplate reader (BioTek Synergy H1 Hybride Multi-mode reader, Agilent technologies, United States) at 450 *nm*. The cytotoxicity value was indicated as cell viability (%). The cell viability was calculated by:

$$Cell\ Viability\ (\%) = [(A_{sample}) - (A_{blank})/(A_{Control}) - (A_{blank})] \times 100\% \quad (4)$$

2.11 Statistical Analysis

Statistical analyses were performed by ImageJ (NIH, USA) and one-way ANOVA in Prism (GraphPad, San Diego, CA, USA). The *p*-values were represented with asterisks (*)

313 are as follows: *ns* > 0.05; **p* <0.05; ***p* <0.01; ****p* <0.001; *****p* <0.0001.
314

315 # 3. Results and Discussion

316 ## 3.1 Membrane morphology and characteristics

317 A blood oxygenation membrane aims to provide sufficient oxygen to the blood. The
318 commercial products and the existing research of ECMO membranes focus on reducing
319 the pore sizes (about 30-40 *nm* diameter) to balance the prevention of blood leakage and
320 the pass of adequate oxygenation [52]. The leakage prevention of the membrane can also
321 be achieved by low surface energy with superhydrophobicity while maintaining sufficient
322 membrane pore sizes. Herein, gradient electrospun nanofiber was prepared as a
323 macroporous membrane. Figure 2a shows that the gradient PCL electrospun membrane
324 comprises two kinds of fiber diameters. The surface layers were fabricated by 9 wt% PCL
325 with 112 *nm* of the mean fiber diameter, which aimed to reduce the membrane mean pore
326 sizes. On the other hand, the middle layer was fabricated by 11 wt% PCL, with a 322 *nm*
327 mean diameter, to provide sufficient mechanical properties.
328 The surface SEM images of the PCL electrospun membrane with different PDMS coating
329 periods (0 min, 30 min, 60 min, 90 min) are shown in Figure 2b. The existence of PDMS
330 after PDMS dip-coating could also be confirmed by EDS analysis (Figure S1), showing
331 that Si was detected on the membrane after PDMS coating. The average membrane
332 thickness of commercial PP and lab-made PMP is 0.133 *mm* and 0.044 *mm*. PCL, PDMS30,
333 PDMS60, and PDMS90 have average membrane thicknesses of 0.199 *mm*, 0.203 *mm*,
334 0.207 *mm*, and 0.210 *mm*, respectively (Figure S5). The coating layer gradually cross-
335 linked on the surface by the increasing coating time from 0 min to 90 min. It is also
336 presented in Figures 2c and 2d that the root mean square surface roughness decreased from
337 0.5038 μm of 0 min coating membrane to 0.1624 μm of 90 min coating samples through
338 AFM scanning. The commercial 0.6 μm polypropylene (PP) Prefilter membrane (Sigma-
339 Aldrich, USA) was purchased to compare the sample properties with those of commercial
340 polymers. Since polymethyl pentene (PMP) did not have a commercial flat film, the lab-
341 made PMP membrane was developed, and the process details are included in the support
342 information. The SEM image of the PMP film and the pore size analysis are listed in the
343 support information (Figure S2).
344 The transmittance spectra of functional groups differences of pristine PCL electrospun
345 membrane and PDMS-treated membrane were acquired through the ATR FTIR

spectrometer (Figure 2e). PCL transmittance showed asymmetric and symmetric stretching vibration of the -CH_2 bond at 2944 and 2866 cm^{-1}. The strong carbonyl (-C=O) stretching band of PCL was represented at around 1726 cm^{-1}. 1295 cm^{-1} indicated C-O and C-C stretching of PCL, and asymmetric and symmetric C-O-C stretching bonds were denoted at 1240 and 1171 cm^{-1} of PCL transmittance. The PDMS-coated membrane showed an intense peak at around 800 cm^{-1} representing the -CH_3 rocking in the Si-CH_3 bond. Si-O-Si bonds of PDMS were shown at 1089 and 1048 cm^{-1}. At the 1240 cm^{-1} band, the PDMS-coated membranes presented more prominent peaks demonstrating the -CH_3 symmetric bending in Si-CH_3. The peak in 2944 cm^{-1} also represented the C-H stretching in the CH_3 group. The spectra proved that after dip-coating, PDMS was successfully cross-linked on the surface of the membrane.

Tensile strength is a critical property of materials. Figure 3a and 3b illustrate tensile stress and strain comparisons, as well as Young's modulus values for different membranes. As the PDMS-coating period was increased, the strain value decreased from 79% of the pristine PCL electrospun membrane to 47% of the PDMS90 membrane. The lower deformation potential reduced the unintentional change in membrane pore size during membrane oxygenation. Meanwhile, the stress value increased from 11 MPa of PCL to 13 MPa of PDMS90, indicating that prolonging the PDMS coating duration enhanced the membrane deformation resistance. Young's modulus improved steadily from 15 MPa of PCL to 25 MPa of PDMS90. The stiffness of the membrane was increased after PDMS dip-coating. Surface roughness and surface chemistry both affect surface hydrophobicity [53]. Based on the water contact angle results (Figure 3c) and the surface roughness results (Figures 2c and 2d), PDMS coating improves the hydrophobicity of the membrane due to the siloxane in the PDMS, from 135.7 degrees of PCL electrospun membrane to 160.2 degree of PDMS60. The decreased surface roughness from 0.29 μm of PDMS60 to 0.16 μm of PDMS90 decreased the water contact angle from 160.2 degrees to 153.3 degrees. At the same time, the blood contact angle of different membranes was measured. According to Figure 3d, as the period of PDMS coating increased, the blood contact angle increased from 121 degrees of PCL to 141 degrees of PDMS90. The surface energies of the membrane were measured by water and ethylene glycol contact angles and computed by the Owens, Wendt, Rabel and Kaelble (OWRK) method. The results are shown in Table 1. As can be observed, the PDMS coating significantly lowered the surface energy of the membranes. Surface energy was correlated to surface roughness and material chemistry [53]. The intrinsic chemical characteristics include atomic composition, polarizability, and

crystallinity. Becauseof the existence of low surface energy elastomer silicone and the low intermolecular interactions betweenthe methyl group, as well as the flexibility of the siloxane backbone, PDMS shows a low surface energy [54] as it is widely known. Therefore, PDMS coating significantly reduced membrane surface energy from over 250 *m*N/*m* before coating to lower than 10 *m*N/*m* after coating.

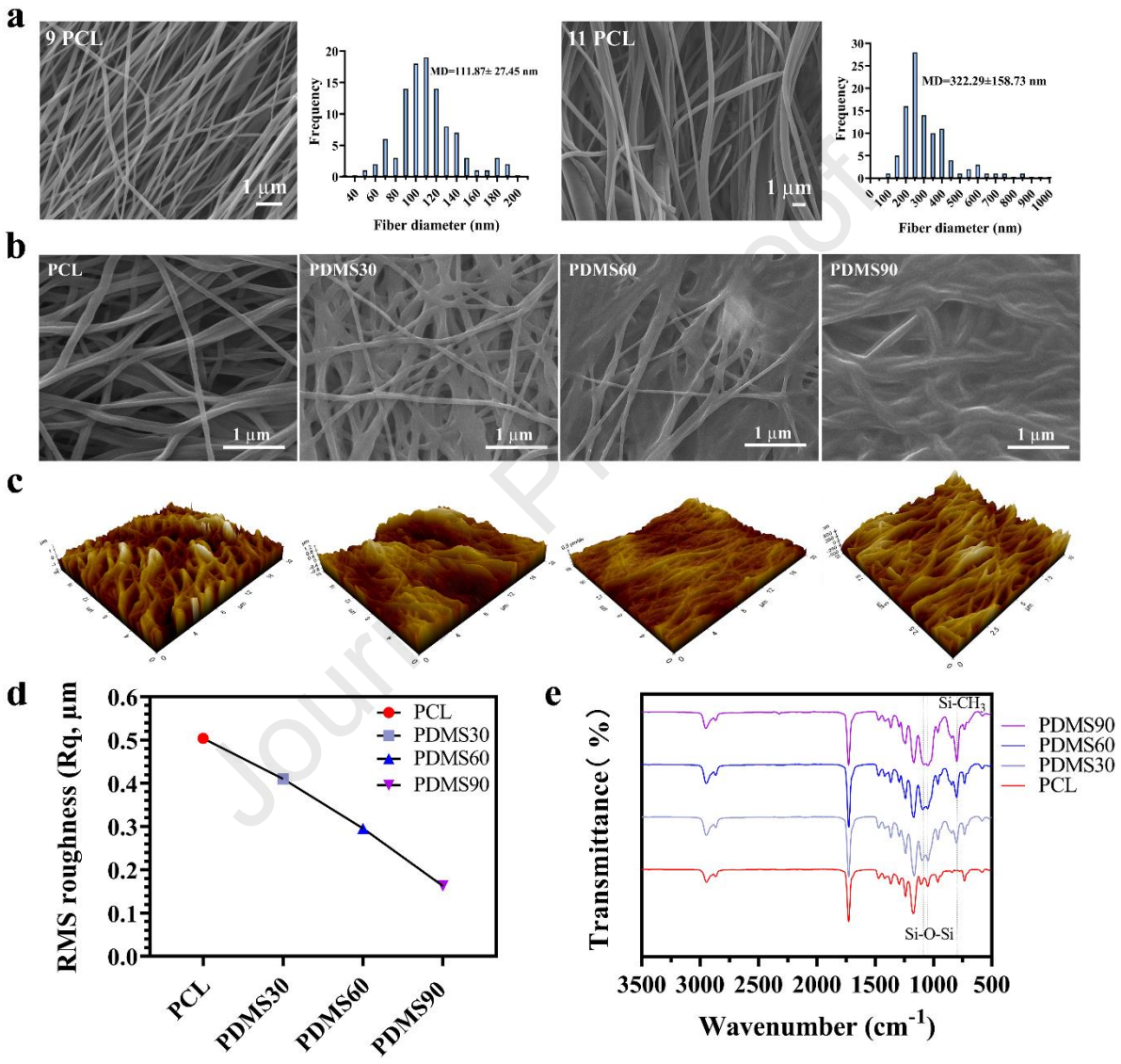

Figure 2. SEM images and fiber diameter analysis of (a) 9 wt% and 11 wt% gradients PCL electrospun membrane; (b) SEMimages and (c) AFM images of membrane surface morphologies with PDMS dip-coating for 0 min (PCL), 30 min (PDMS30), 60 min (PDMS60) and 90 min (PDMS90); (d) the surface roughness analysis; and (e) ATR-FTIR examination of PCL, PDMS30, PDMS60, and PDMS90 membranes.

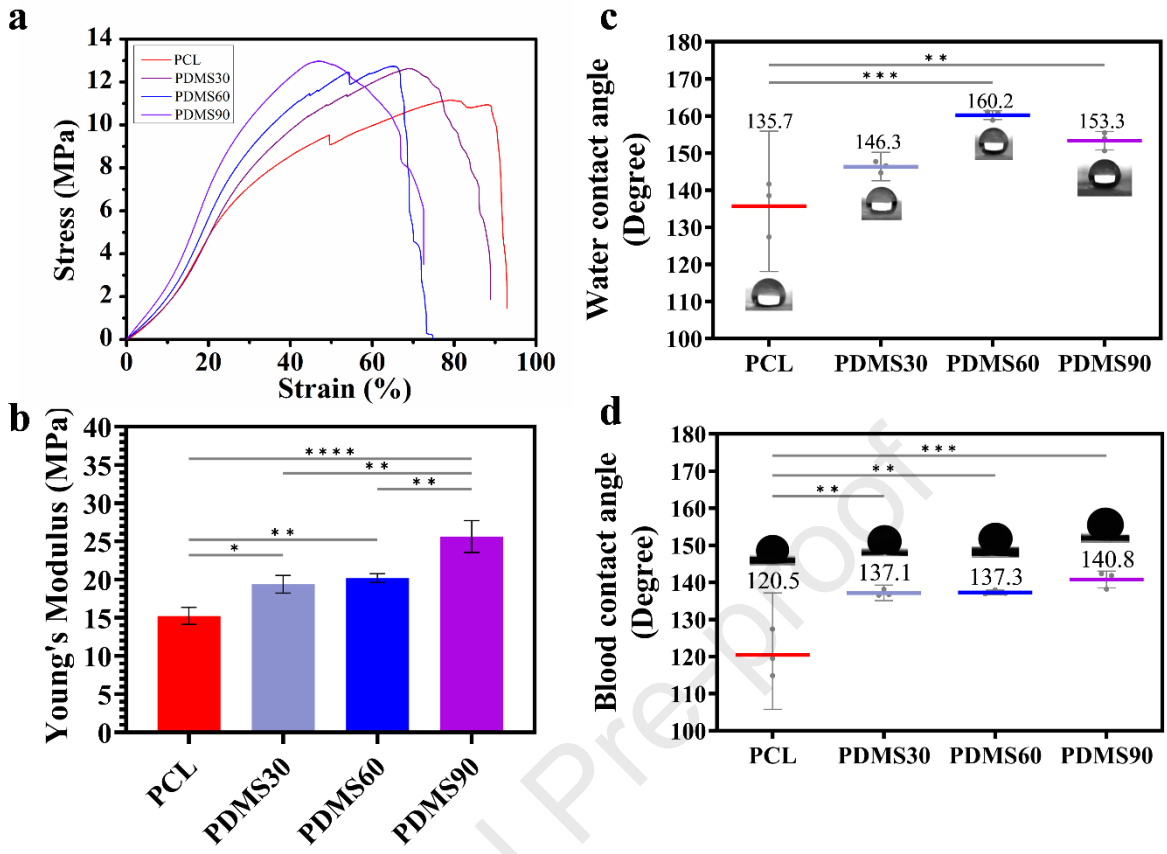

Figure 3. (a) The mechanical properties and (b) Young's modulus of PCL, PDMS30, PDMS60, and PDMS90 membranes. (c) Water contact angle and (d) blood contact angle of PCL, PDMS30, PDMS60, and PDMS90 membranes.

Membranes	Contact angle (degree)		Surface energy (mN/m)
	Water	Ethylene glycol	
PCL	135.7	28.88	251.2
PDMS30	146.3	125.67	6.70
PDMS60	160.2	139.82	3.62
PDMS90	153.3	130.97	6.36

Table 1. The comparison of contact angles and surface energy of different membranes.

3.2 Hemocompatibility of the membrane

3.2.1 Hemolysis assay

Since the ECMO membrane comes into direct touch with the patient's blood, membrane hemocompatibility must be investigated. Hemolysis appears when blood directly contacts the foreign elements that may activate the complement system and results in inflammation.

The hemolysis ratio may reflect a material's blood compatibility. The in vitro hemolysis assay showed that all samples, including commercial PP and lab-made PMP, had average hemolysis ratios of less than 0.6%. (Figure 4a). The results show that all the samples are comparably safe for in vitro hemolysis tests, in accordance with the American Society for Testing and Materials Standard (ASTM F756-2008). PCL, PDMS30, and PDMS60 had higher hemolysis ratios than commercial PP and lab-made PMP, whereas commercial PP and lab-made PMP had hemolysis rates less than 0.4%. PDMS90 had an excellent hemolysis ratio of 0.22% on average, which was lower than lab-made PMP (0.24%). Among the tested samples, the PDMS90 membrane showed the best hemocompatible capability, suggesting that the hemocompatible PDMS90 has the potential for ECMO application.

3.2.2 Blood Clotting Index

The blood clotting index (BCI) assesses clotting formation capacity, which reveals the percentage of red blood cells that are not caught by clots. A lower BCI level indicates that the materials are significantly prone to clotting. According to figure 4b, the average BCI value for pristine PCL electrospun membrane was lower than 90%. The BCI tended to grow as the PDMS-coating duration increases. PDMS90 had a BCI value of more than 95%, which was comparable to the commercial PP membrane (96.6%). Since PDMS90 had a lower clotting potential, platelet plugs and fibrin clots were less likely to form on the membrane. Meanwhile, the oxygenation tunnel might work better for a longer period with less clogging. The results suggest that PDMS90 could be employed as an ECMO membrane with minimal clotting potential.

3.2.3 Protein adsorption

After the blood directly contacts an artificial surface, protein adsorption appears in a matter of seconds as a forepart reaction. Proteins have a significantly smaller size than cells, which causes them to adhere to the microscopic structure more than cells. When a large number of proteins are bound to the surface, the artificial surface may activate blood cells and cause thrombosis [55]. Meanwhile, the adhesive proteins have a proclivity for cell attraction, which will eventually block the oxygenation tunnel and limit the ECMO membrane's oxygenation rate [24]. The difficulty in modifying ECMO membrane surfaces is lowering protein adhesion to prevent further thrombosis and increase service life. In figure

4c, all membrane samples were examined for 3, 6, and 9 hours with a high concentration of 10 *m*g/*m*L bovine serum albumin. At 3 hours of incubation, PDMS90 (0.85 $\mu g/cm^2$) revealed less than 1 $\mu g/cm^2$, indicating effective protein adsorption avoidance. Protein adsorption of the membranes fell considerably after PDMS coating, from over 100 $\mu g/cm^2$ of pristine PCLelectrospun membrane to less than 10 $\mu g/cm^2$ of PDMS-coated membrane at 9 hours (PDMS30: 6.31 $\mu g/cm^2$, PDMS60: 4.99$\mu g/cm^2$, PDMS90: 3.87$\mu g/cm^2$). When compared to commercial PP and lab-made PMP membranes, the PDMS-modified membrane showed a significant reduction in protein adsorption, with less than half of PP and PMP after 9 hours of incubation. Figure 5 reviews various membranes applied to ECMO machines and antifouling bio-interfaces. It presents that this work (PDMS90) has a low protein adsorption amount under the incubation of relatively high BSA concentration (10 *mg*/*m*L), which stands out from other works. The membranes have been repeatedly tested with 1 *mg*/*m*L of BSA concentration for 3, 6, and 9 hours (Figure S6). It shows that PDMS90 possesses lower than 1.5 $\mu g/cm^2$ protein adsorption after 9 hours of incubation with 1 *mg*/*m*L BSA solution. The details of figure 5 are listed in table S1. The results demonstrate that the superhydrophobicity and the relative roughness of the PDMS-coated membrane surface inhibited protein adhesion, and the low protein adsorption membrane has the potential to apply to the ECMO membrane.

3.2.4 Cytotoxicity

Because the ECMO membrane is in direct touch with the blood extracted from the venous vessels, the blood will return to the patient's body via the arterial channel. The membrane's safety is also critical. According to the biological assessment of medical devices (ISO10993-5), Cell Counting Kit-8 (CCK-8) was used to examine the in vitro cytotoxicity of the ECMO membrane using Human Umbilical Vein Endothelial Cells (HUVEC). The cytotoxic potential of materials such as PCL, PDMS90, commercial PP, and lab-made PMP wasinvestigated (Figure 4d). The cell viability of several samples was tested for 24 hours, 48 hours, and 96 hours in the non-antibiotic-free medium. Based on the conventional quantitative level (ISO 10993-5:2009), at 24 hours, PCL had 75.8% cell viability, lab-made PMP had 80.7%, and PDMS90 had 84.9% viability. PCL, PMP, and PDMS90 membranes were defined as level 1 cytotoxicity after 24 hours. Commercial PP (71.5%) had the lowest cell viability and was defined as level 2 cytotoxicity at 24 hours. Only PDMS90 retained more than 80% cell viability after 48 hours, followed by 78.86% for

PMP, 69.08% for PP, and 66.3% for PCL. At 48 hours, PDMS90 and PMP still showed level 1 cytotoxicity, but PP and PCL demonstrated level 2 cytotoxicity. PMP (75%) presented the best cytotoxicity after 72 hours with level 1 cytotoxicity. At 72 hours, PDMS90 (59.7%) demonstrated level 2 cytotoxicity, while PCL (40.94%) and PP (31.38%) showed level 3 cytotoxicity. The results suggest that PDMS90 might be used as a medical device, but it may require further treatment to lessen the cytotoxic potential in the long-term application.

3.2.5 Platelet adhesion

Platelets are anucleate blood cells that might participate in inflammation during extracorporeal membrane oxygenation [26]. When the membrane encounters blood, proteins (albumins and globulins) tend to bind to the membrane surface. After that, fibrinogens gradually replace small proteins and attach to the membrane surface due to the Vroman effect [56]. Platelets tend to aggregate in the presence of fibrinogens. Subsequently, the platelet will be activated and spread the pseudopodia. Furthermore, the extent of platelet activation on ECMO might improve with increasing blood contact time, resulting in a membrane with a low oxygenation efficiency. For the platelet adhesion test, extracted sheep platelets were utilized — platelet diameters in sheep range from 3.2 to 5.4 $f\mathrm{L}(\mu m^3)$ [57]. Figure 4e depicts the platelet formed on various membrane surfaces. The platelet on the pristine PCL electrospun membrane surface had been activated with multiple pseudopodia. Through SEM pictures, the platelet appeared reductive activation as the PDMS coating time increased. A platelet on the surface of a commercial PP membrane was severely activated. In contrast, a platelet on the surface of a lab-made PMP membrane was hardly activated, which was similar to the PDMS90 surface platelet. The platelet adhesion is also related to material surface roughness [58]. PDMS dip-coating reduced the surface roughness (Figure 2d), which conduce to less platelet adhesion on the membrane surface. Hence, the surface was modified into superhydrophobic with relatively lower surface roughness and minimal protein adsorption, PDMS coating reduced platelet activation and could potentially extend service life in ECMO applications.

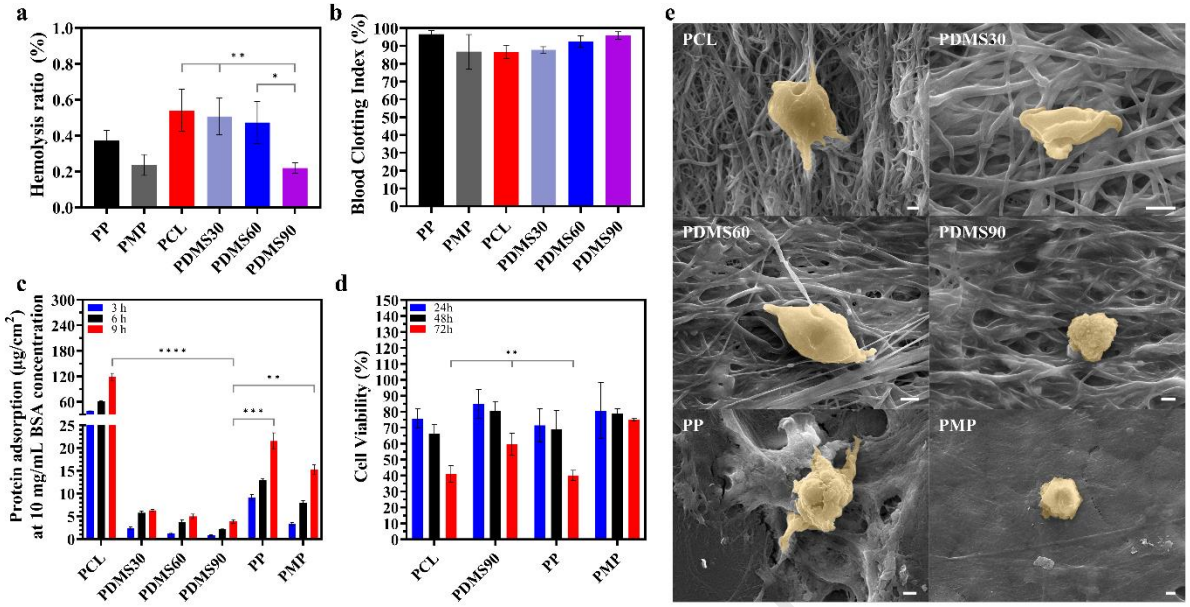

Figure 4. Hemocompatibility evaluation of PCL, PDMS30, PDMS60, PDMS90, commercial PP, and lab-made PMP: (a) hemolysis ratios (b) the corresponding blood clotting index values (c) protein adsorption of membranes with 10 *mg*/*m*L BSA concentration at 3, 6, 9 hours respectively; (d) cytotoxicity analysis of PCL, PDMS60, commercial PP, and lab-made PMP membranes by the cell viability for 24, 48, 72 hours respectively. (e) SEM images of surface platelet activation for PCL, PDMS30, PDMS60, PDMS90, commercial PP, and lab-made PMP membranes. (Scale bar: 1 μm.)

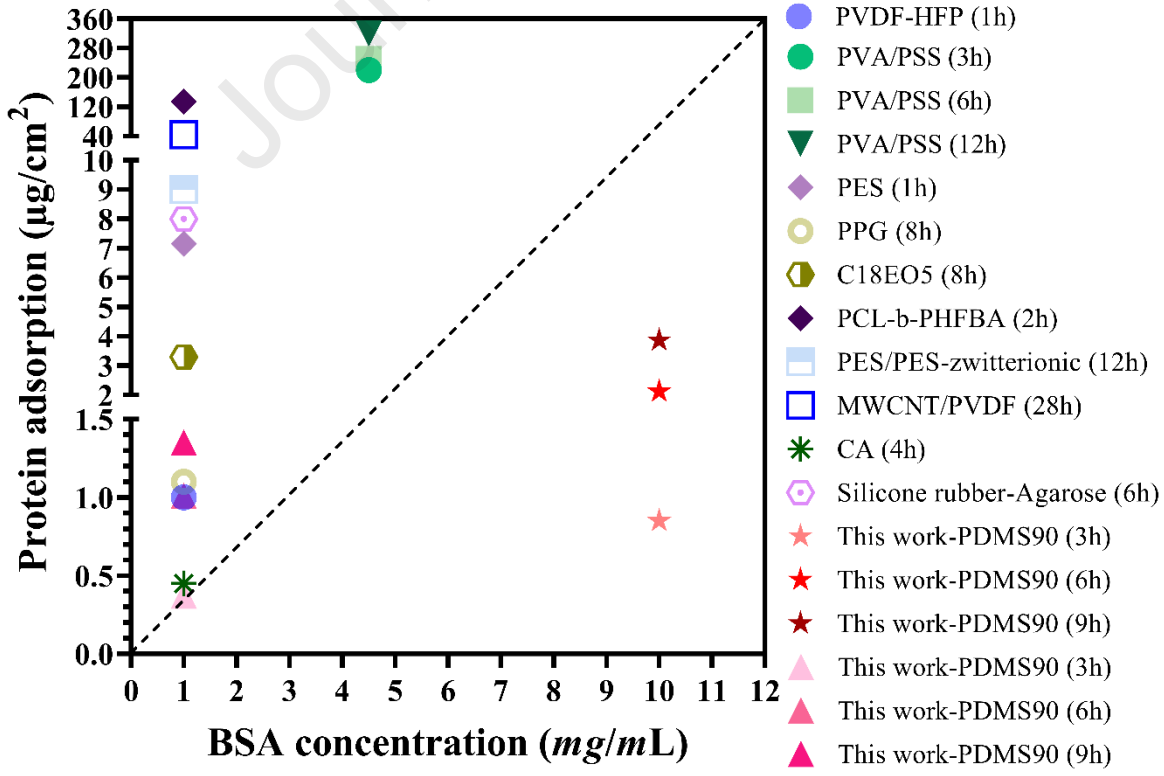

Figure 5. The comparison of protein adsorption of various membranes applied to ECMO and bio-interfaces (details are listed in Figure S6 and Table S1).

3.2.6 Long-term antifouling

The superhydrophobicity of the ECMO membrane is designed to extend the lifetime of respiratory assistance. The long-term antifouling ability of the membrane surface is also crucial; by reducing cell adhesions over time, oxygenation could theoretically persist longer. The membrane samples were steeped in citrated sheep blood for 28 days in this study to test long-term antifouling properties. The antifouling ability of the membrane surfaces was observed by SEM at 7-day intervals and photography at 28-day (Figure 6).

From photography, the PCL and commercial PP membranes had significant clotting on the surface, as observed in the 28-day image. In contrast, the PDMS-coated membrane surfaces were comparable to the fresh membrane (control). After 28 days of blood interaction, the lab-made PMP membrane likewise had a clean surface. Simultaneously, SEM pictures of PCL and commercial PP membrane surfaces indicated incremental thrombus buildup at 28 days, the PP membrane surface accumulated activated platelets from day 14, and the PCL electrospun membrane showed active platelets from day 21. PDMS-coated membranes and lab-made PMP demonstrated better antifouling characteristics. The increased coating duration from PDMS30 to PDMS90 delivered a preferable antifouling feature to the membrane. Meanwhile, PDMS60 and PDMS90 exhibited similar antifouling capabilities to lab-made PMP membranes with nearly free of thrombus and activated platelets. The results demonstrate that the PDMS coating significantly increased the membrane's long-term anticoagulant property. The competitive performance might be traced to the inert siloxane of the PDMS coating layer, which enabled the membrane with low surface energy and superhydrophobicity. The superhydrophobic surface collected less protein from the blood, which reduced both platelet activation and erythrocyte adherence, resulting in a longer-term possibility of anticoagulation.

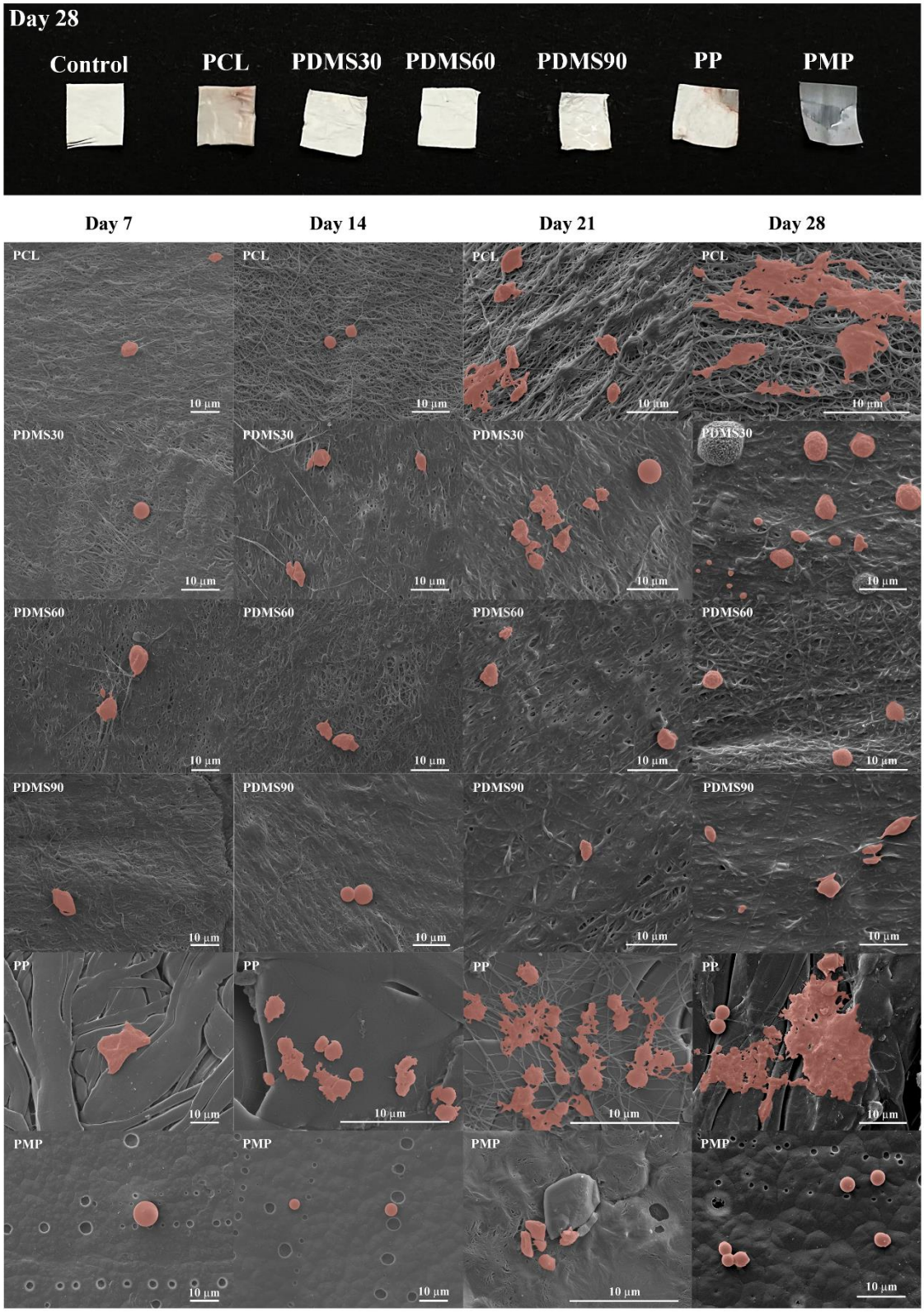

Figure 6. (Top) 28 days antifouling examination of membranes (Control: Non-blood contacted clean PDMS60 membrane, PCL, PDMS30, PDMS60, PDMS90, commercial PP, and lab-made PMP); (Bottom) SEM micrographs of membranes after citrated sheep blood incubation for 7, 14, 21, 28 days respectively.

3.3 Membrane Blood Oxygenation

The pore size of the membrane may influence the rate of oxygenation. The mean pore diameter of a commercial PP membrane (Sigma-Aldrich, USA) was 0.6 μm, and the mean pore size of a lab-made PMP was 1.74 μm (Figure S2). Meanwhile, the PCL electrospun membrane had a mean flow pore diameter of 261.6 *nm*, 334.5 *nm* for PDMS30, 276.5 *nm* for PDMS60, and 213.4 *nm* for PDMS90, respectively (Figure 7a). Among them, the rising pore size of PDMS30 was due to the capillary effect that accumulated the nanofiber clusters during PDMS dip-coating. When the dry membrane was submerged in the coating solution, the nanofibers of the membrane tended to aggregate owing to the cohesiveness between liquid and solid [59][60]. The steady decrease in pore sizes of PDMS60 and PDMS90 was linked to the enhancement of the PDMS cross-linking degree, which was well-distributed across the membrane surface and reduced pore sizes [61].

Gas permeance is also affected by pore size and membrane interior structure. All the test samples had an air permeance greater than 2.7×10^5 GPU. Whereas commercial PP had 1.56×10^4 GPU of air permeance, lab-made PMP had 4.27×10^2 GPU [52]. Figure 7b indicates that the PDMS-coated membrane significantly lowered air permeance, and it was owing to the denser interior structure. The PCL electrospun membrane had a loose internal structure prior to coating, and the PDMS coating method not only assembled the surface nanofiber but also congregated the fibers between various layers. Therefore, the overall air permeation channel had been diminished, and the air permeance of the PDMS90 membrane decreased dramatically to 2.7×10^5 GPU. However, as compared to other products [25][26], these tested samples still had good air permeability.

The hydrophobicity of a PCL electrospun membrane was enhanced to superhydrophobicity by PDMS coating. The goal of membrane superhydrophobicity was to avoid blood leakage during blood oxygenation. To test the wetting stability of the membrane, the membranes were pre-fixed under the water for 24 hours before applying pressure. The liquid entry pressure (LEP) of a hydrophobic membrane is the pressure required to pass the liquid through a membrane. According to Figure 7c, when the PDMS coating duration increased, the LEP increased from 0 *bar* of PCL to 1.625 *bar* of PDMS90. Even though the electrospun PCL membrane has over 135 degrees of water contact angle, it showed 0 bar after 24 hours of pre-wetting. This result could be due to the free arrangement of electrospun fiber that allows the water to pass through in long-term

contact with water. The increasing LEP value is bounded up with the decreasing pore size, the increasing thickness of the membrane, and the improving hydrophobicity by the PDMS dip-coating. Consequently, the possibility of blood leakage through the membrane pores was reduced as compared to the PCL electrospun membrane, and the blood oxygen exchange tunnel was less likely to get clogged because of improved hydrophobicity.

A membrane oxygenator has gas flowing at the interior of the gas exchange hollow fiber, and the blood is pumped to flow around the exterior of the hollow fibers. The O_2/CO_2 exchanges during the flow, and the blood is latterly led back to the patient's body after the oxygenation. A dead-end system is applied to target the membrane oxygen transfer rate using Amicon® cells to avoid undesired influences for testing membrane oxygenation efficiency. The membrane separated the flown gas and the gently stirred blood, and the O_2/CO_2 was exchanged through the membrane pores and the gas permeability of the materials. The oxygen level of sheep blood was measured from under 70% in 5 minutes intervals and recorded until it reached over 95%. Figure 7d and 7e compare the blood oxygenation simulation efficiency of commercial PP, lab-made PMP, and PDMS-coated membranes. Among the tests, commercial PP (6.16 *m*L $O_2/m^2/min$) had the highest oxygen exchange rate, whereas dense lab-made PMP (3.53 *m*L $O_2/m^2/min$) had the lowest value. Because the PCL electrospun membrane was not superhydrophobic that cannot prevent blood leakage over the period, it was ineligible for the blood oxygenation simulation test. PDMS had superior intrinsic oxygen and carbon dioxide gas permeability when compared to commercial PP and lab-made PMP polymers [62][63]. The increasing coating duration of PDMS offered a more competitive oxygenation efficiency to the membranes (4.66 *m*L $O_2/m^2/min$ of PDMS30, 4.95 *m*L $O_2/m^2/min$ of PDMS60, and 5.74 *m*L $O_2/m^2/min$ of PDMS90). The blood oxygen saturation level revealed that PP and PDMS90 met at 20 minutes with an 88% blood saturation level and continued to increase at the same rate from 20 minutes to 30 minutes until exceeding 95% of the oxygen saturation level, where the normal oxygen level in a healthy lung is between 95% and 100% [64]. Figure S3 shows the tested sheep blood was completely removed from the surface of the PDMS30, PDMS60, and PDMS90 membranes, by gentle distilled water rinsing after the membranes had completed deoxygenation and blood oxygenation tests. The clean surfaces also demonstrate the PDMS-coated antifouling membranes could have promising and stable blood oxygenation properties without thrombus adhesion. As a result, according to the saturation level test, PDMS90 was competitive with commercial PP membranes that had

the same saturation speed to achieve 97% at 30 minutes during the test. The oxygenation characteristics of a PDMS-coated PCL electrospun membrane were comparable to those of commercial PP and lab-made PMP membranes. As a competitor, PDMS-coated PCL electrospun membrane has enormous blood oxygenation potential to be utilized for ECMO membranes.

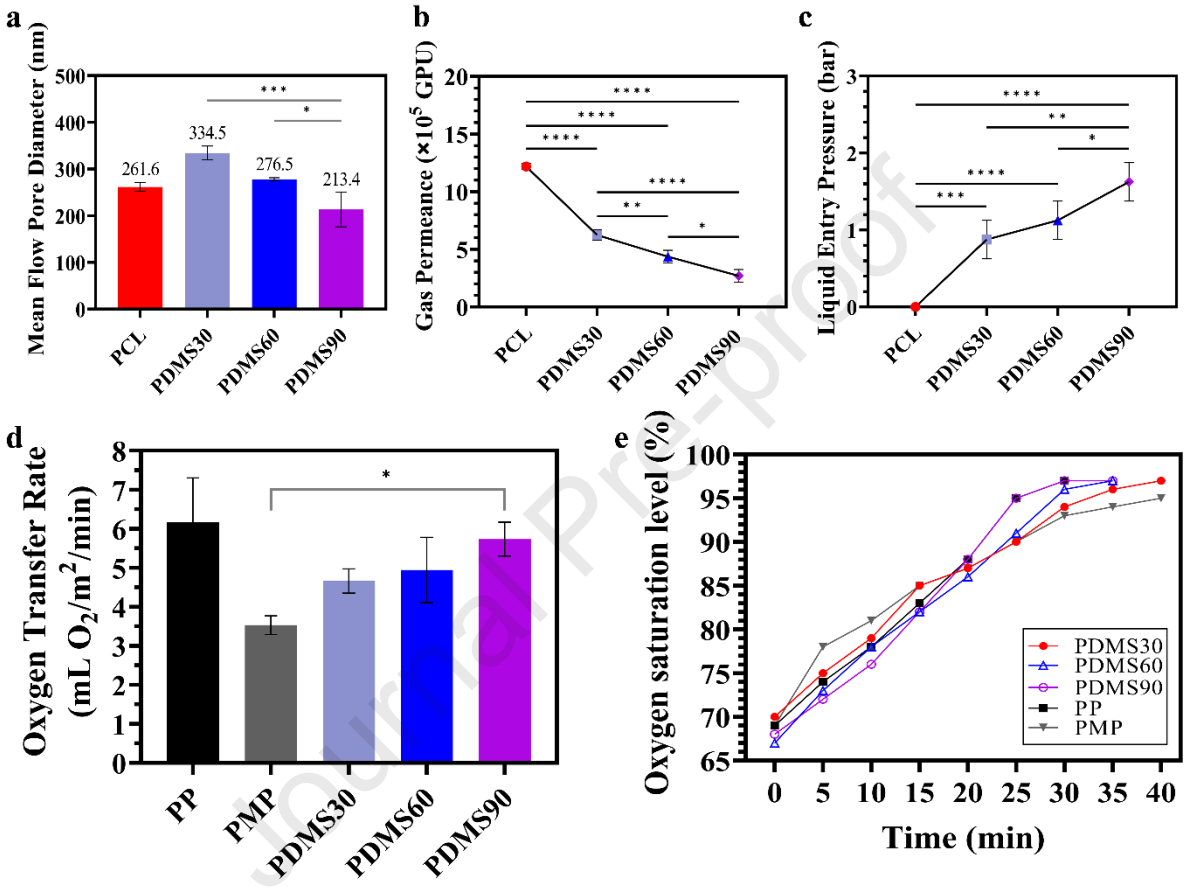

Figure 7. (a) Mean pore diameter distribution and corresponding (b)air permeances and (c)Liquid Entry Pressure (LEP)of PCL, PDMS30, PDMS60, and PDMS90. (d) Oxygen transfer rate and (e) oxygen saturation level of PP, PMP, PDMS30, PDMS60, PDMS90.

4. Conclusions

In this work, we created a PCL electrospun membrane with a PDMS dip-coated superhydrophobic surface. Two different concentration solutions (9 wt% and 11 wt%) were prepared to produce a gradient PCL electrospun membrane to form a hydrophobic porous membrane. PDMS dip-coating lifts the water contact angle from 135 degrees to 160 degrees, enhancing the membrane's long-term antifouling. The PDMS dip-coating also improves the hemocompatibility of the membrane. Under 10 *m*g/*m*L BSA concentration, the protein

adsorption of the membrane dramatically reduces from 118 $\mu g/cm^2$ of PCL electrospun membrane to 3.9 $\mu g/cm^2$ of PDMS90 at 9 hours incubation. The protein adsorption of PDMS90 was also lower than the commercial PP and lab-made PMP membranes. Less protein adsorption of the membrane surface further depresses the platelet activation and improves the long-term antifouling property. PDMS dip-coated PCL electrospun membrane also shows competitive blood oxygenation performance. PDMS90 meets PP at 20 min with an 88% oxygen saturation level; after that, keeping the same speed as PP and reaches 97% at 30 min. Meanwhile, the gas transfer rate of PDMS90 is 5.7 $mL\ O^2/m^2/min$, which is competitive with 6.16 $mL\ O^2/m^2/min$ of commercial PP membrane. Compared to the most often used materials for ECMO membranes, the PDMS-coated PCL electrospun membrane is comparable to the hemocompatibility of lab-made PMP membranes and competitive with the blood oxygenation capability of commercial PP membranes. Thus, the PDMS-coated PCL electrospun membrane exhibits superior overall performance, indicating its potential for ECMO application. For the next step of developing the PDMS dip-coated PCL electrospun membrane for ECMO application, the collector could be adjusted to a small diameter cylinder to get the hollow-shaped tube, which could test and simulate the blood flow, shear force, and pressure in the hollow tube oxygenator in the future. Surface superhydrophobic modification by FDA- approved materials could also benefit various blood-directly-contacting medical interfaces, such as blood vessel grafts, blood tubes, and blood reservoirs.

Author statement

Zhuomin Jiang: Conceptualization, Methodology, Data analysis, Writing-original draft, Writing-review & editing. **Bao Tran Duy Nguyen**: Methodology, Data analysis. **JeongHyeon Seo**: Methodology, Data analysis. **Changgi Hong**: Methodology, Data curation. **Dongwoo Kim**: Methodology, Data curation. **Suhyun Ryu**: Data curation. **Sohui Lee:** Data curation. **Gyubok Lee:** Data curation. **Young Hoon Cho:** Review & Editing, Validation, Resources. **Jeong F. Kim:** Review & Editing, Validation, Resources. **Kangwon Lee:** Supervision, Funding acquisition, Project administration.

Declaration of competing interest

The authors declare no conflicts of interest.

Acknowledgements

This work was in part supported by the Research Institute for Convergence Science, Graduate School of Convergence Science and Technology and Research Institute of Advanced Materials, Seoul National University. This work was supported by the Ministry of Trade, Industry and Energy (20018522, 20010846). This work was supported by a grant from the Korea Health Technology R&D Project through the Korea Health Industry Development Institute (KHIDI), funded by the Ministry of Health and Welfare, Republic of Korea (grant number: HI22C1394, HI22C1234). This work was also conducted with the support of the Ministry of Science and ICT (SI2211-40, KRICT).

Appendix A. Sample Appendix Section

EDS analysis of PCL electrospun membrane before and after PDMS dip-coating. SEM image and pore size analysis of lab-made PMP membrane. The fabrication instruction of lab-made PMP membrane. Photograph of various PDMS dip-coated membranes after blood oxygenation tests and the surface with a gentle distilled water rinse. The comparison of various low protein adsorption membranes for ECMO and bio-interfaces.

References

[1] A. Vuylsteke, Ecmo in covid-19: do not blame the tool, The Lancet398 (10307) (2021) 1197–1199. https://doi.org/10.1016/s0140-6736(21)02137-1

[2] J. Badulak, M. V. Antonini, C. M. Stead, L. Shekerdemian, L. Raman, M. L. Paden, C. Agerstrand, R. H. Bartlett, N. Barrett, A. Combes, R. Lorusso, T. Mueller, M. T. Ogino, G. Peek, V. Pellegrino, A. A. Rabie, L. Salazar, M. Schmidt, K. Shekar, G. MacLaren, D. Brodie, Extracorporeal membrane oxygenation for covid-19: Updated 2021guidelines from the extracorporeal life support organization, ASAIOJournal 67 (5) (2021) 485–495. https://doi.org/10.1097/mat.0000000000001422

[3] G. Martinez, A. Vuylsteke, Extracorporeal membrane oxygenation inadults, Continuing Education in Anaesthesia Critical Care Pain 12 (2) (2011) 57–61. https://doi.org/10.1093/bjaceaccp/mkr056

[4] W. J. Federspiel, K. A. Henchir, Lung, artificial: basic principles and current applications, Encyclopedia of biomaterials and biomedical engineering 9 (2004) 910. DOI:10.1201/b18990-161

[5] J. M. t. Daniel, P. A. Bernard, S. C. Skinner, P. Bhandary, A. Ruzic, M. K. Bacon, H. O. Ballard, Hollow fiber oxygenator composition has a significant impact on failure rates in neonates on extracorporeal membrane oxygenation: A retrospective analysis, J Pediatr Intensive Care7 (1) (2018) 7–13. https://doi.org/10.1055/s-0037-1599150

[6] C. M. Zimmerman, A. Singh, W. J. Koros, Tailoring mixed matrix composite membranes for gas separations, Journal of Membrane Science 137 (1) (1997) 145–154. https://doi.org/10.1016/S0376-7388(97)00194-4

[7] L. W. Lund, B. G. Hattler, W. J. Federspiel, Is condensation thecause of plasma leakage in microporous hollow fiber membrane oxygenators, Journal of Membrane Science 147 (1) (1998) 87–93. https://doi.org/10.1016/S0376-7388(98)00121-5

[8] B. P. Nguyen Thi, B. T. Duy Nguyen, I.-S. Jeong, J. F. Kim, Hemocompatibility challenge of membrane oxygenator for artificial lung technology, Acta Biomaterialia 152 (2022) 19–46. https://doi.org/10.1016/j.actbio.2022.09.003

[9] Y. Feng, Q. Wang, L. Zhi, S. Sun, C. Zhao, Anticoagulant biomimetic consecutive gas exchange network for advanced artificial lung membrane, Journal of Membrane Science 653 (2022) 120502. https://doi.org/10.1016/j.memsci.2022.120502

[10] L. Zhi, S. Li, X. He, Y. Feng, C. Cheng, S. Li, S. Sun, C. Zhao, In-situ modified polyethersulfone oxygenation membrane with improved hemocompatibility and gas transfer efficiency, Journal of Membrane Science 667 (2023) 121162. https://doi.org/10.1016/j.memsci.2022.121162

[11] F. Hesselmann, N. Scherenberg, P. Bongartz, S. Djeljadini, M. Wessling, C. Cornelissen, T. Schmitz-Rode, U. Steinseifer, S. V. Jansen, J. Arens, Structure-dependent gas transfer performance of 3D-membranes for artificial membrane lungs, Journal of Membrane Science 634 (2021) 119371. https://doi.org/10.1016/j.memsci.2021.119371

[12] Rv, E. K. Bassett, D. M. Hoganson, J. P. Vacanti, K. K. Gleason, Ultra-thin, gas permeable free-standing and composite membranes for microfluidic lung assist devices, Biomaterials 32 (16) (2011) 3883–3889. https://doi.org/10.1016/j.biomaterials.2011.02.017

[13] R. Bagherzadeh, S. S. Najar, M. Latifi, M. A. Tehran, L. Kong, A theoretical analysis and prediction of pore size and pore size distribution in electrospun multilayer nanofibrous materials, Journal of Biomedical Materials Research Part A 101A (7) (2013) 2107–2117. https://doi.org/10.1002/jbm.a.34487

[14] D. Li, M. W. Frey, Y. L. Joo, Characterization of nanofibrous membranes with capillary flow porometry, Journal of Membrane Science 286 (1) (2006) 104–114. https://doi.org/10.1016/j.memsci.2006.09.020

[15] S. Lee, S. K. Obendorf, Use of electrospun nanofiber web for protective textile materials as barriers to liquid penetration, Textile research journal 77 (9) (2007) 696–702. https://doi.org/10.1177/0040517507080284

[16] S. Soliman, S. Pagliari, A. Rinaldi, G. Forte, R. Fiaccavento, F. Pagliari, O. Franzese, M. Minieri, P. Di Nardo, S. Licoccia, E. Traversa, Multiscale three-dimensional scaffolds for soft tissue engineering via multimodal electrospinning, Acta Biomaterialia 6 (4) (2010) 1227–1237.https://doi.org/10.1016/j.actbio.2009.10.051

[17] F.-L. He, D.-W. Li, J. He, Y.-Y. Liu, F. Ahmad, Y.-L. Liu, X. Deng,Y.-J. Ye, D.-C. Yin, A novel layer-structured scaffold with large pore sizes suitable for 3D cell culture prepared by near-field electrospinning, Materials Science and Engineering: C 86 (2018) 18–27. https://doi.org/10.1016/j.msec.2017.12.016

[18] X. Huang, W. Wang, Z. Zheng, W. Fan, C. Mao, J. Shi, L. Li, Surface monofunctionalized polymethyl pentene hollow fiber membranes by plasma treatment and hemocompatibility modification for membrane oxygenators, Applied Surface Science 362 (2016) 355–363. https://doi.org/10.1016/j.apsusc.2015.11.236

[19] Y. Liu, G. Li, Q. Han, H. Lin, Q. Li, J. Hua, F. Liu, Anticoagulantdialyzer with enhanced ca2+ chelation and hydrophilicity for heparin free hemodialysis, Journal of Membrane Science 604 (2020) 118082. https://doi.org/10.1016/j.memsci.2020.118082

[20] T. Oto, F. Rosenfeldt, M. Rowland, A. Pick, M. Rabinov, A. Preovolos, G. Snell, T. Williams, D. Esmore, Extracorporeal membrane oxygenation after lung transplantation: Evolving technique improves outcomes, The Annals of Thoracic Surgery 78 (4) (2004) 1230–1235.

https://doi.org/10.1016/j.athoracsur.2004.03.095

[21] Y. Shen, W. Zhao, K. Xiao, X. Huang, A systematic insight into fouling propensity of soluble microbial products in membrane bioreactors based on hydrophobic interaction and size exclusion, Journal of Membrane Science 346 (1) (2010) 187–193. https://doi.org/10.1016/j.memsci.2009.09.040

[22] W. Zimmerli, P. Sendi, Pathogenesis of implant-associated infection: the role of the host, Seminars in Immunopathology 33 (3) (2011) 295–306. https://doi.org/10.1007/s00281-011-0275-7

[23] I. H. Jaffer, J. C. Fredenburgh, J. Hirsh, J. I. Weitz, Medical device-induced thrombosis: what causes it and how can we prevent it?, Journal of Thrombosis and Haemostasis 13 (S1) (2015) S72–S81. https://doi.org/10.1111/jth.12961

[24] M. B. Gorbet, M. V. Sefton, Biomaterial-associated thrombosis: roles of coagulation factors, complement, platelets and leukocytes, Biomaterials 25 (26) (2004) 5681–5703. https://doi.org/10.1016/j.biomaterials.2004.01.023

[25] Y. Wang, Y. Liu, Q. Han, H. Lin, F. Liu, A novel poly (4-methyl-1-pentene)/polypropylene (PMP/PP) thin film composite (TFC) artificiallung membrane for enhanced gas transport and excellent hemo-compatibility, Journal of Membrane Science 649 (2022) 120359.https://doi.org/10.1016/j.memsci.2022.120359

[26] E. Yi, H. S. Kang, S. M. Lim, H. J. Heo, D. Han, J. F. Kim, A. Park, D. H. Choi, Y.-I. Park, H. Park, Y. H. Cho, E.-H. Sohn, Superamphiphobic blood-repellent surface modification of porous fluoropolymer membranes for blood oxygenation applications, Journal of Membrane Science 648 (2022) 120363. https://doi.org/10.1016/j.memsci.2022.120363

[27] A. Ontaneda, G. M. Annich, Novel surfaces in extracorporeal membrane oxygenation circuits, Frontiers in Medicine 5 (2018). https://doi.org/10.3389/fmed.2018.00321

[28] M. Zhang, C. H. H. Chan, J. P. Pauls, C. Semenzin, C. Ainola, H. Peng, C. Fu, A. K. Whittaker, S. Heinsar, J. F. Fraser, Investigation of heparin-loaded poly (ethylene glycol)-based hydrogels as antithrombogenic surface coatings for extracorporeal membrane oxygenation, Journal of Materials Chemistry B 10 (26) (2022) 4974–4983. http://dx.doi.org/10.1039/D2TB00379A

[29] M. Pieri, O. G. Turla, M. G. Calabrò, L. Ruggeri, N. Agracheva, A. Zangrillo, F. Pappalardo, A new phosphorylcholine-coated poly-methyl pentene oxygenator for extracorporeal membrane oxygenation: a preliminary experience, Perfusion 28 (2) (2013) 132–7. https://doi.org/10.1177/0267659112469642

[30] H. Suhara, Y. Sawa, M. Nishimura, H. Oshiyama, K. Yokoyama, N. Saito, H. Matsuda, Efficacy of a new coating material, PMEA, for cardiopulmonary bypass circuits in a porcine model, The Annals of Thoracic Surgery 71 (5) (2001) 1603–1608.

https://doi.org/10.1016/S0003-4975(01)02466-3

[31] T. He, S. Yu, J. He, D. Chen, J. Li, H. Hu, X. Zhong, Y. Wang, Z. Wang, Z. Cui, Membranes for extracorporeal membrane oxygenator (ECMO): History, preparation, modification and mass transfer, Chinese Journal of Chemical Engineering 49 (2022) 46–75. https://doi.org/10.1016/j.cjche.2022.05.027

[32] X. Yao, Y. Liu, Z. Chu, W. Jin, Membranes for the life sciences and their future roles in medicine, Chinese Journal of Chemical Engineering 49 (2022) 1–20. https://doi.org/10.1016/j.cjche.2022.04.027

[33] T. He, J. He, Z. Wang, Z. Cui, Modification strategies to improve the membrane hemocompatibility in extracorporeal membrane oxygenator(ECMO), Advanced Composites and Hybrid Materials 4 (4) (2021) 847– 864. https://doi.org/10.1007/s42114-021-00244-x

[34] L.-L. Bao, H.-Q. Huang, J. Zhao, K. Nakashima, Y.-K. Gong, Preparation and characterization of zwitterionic phospholipid polymer- coated poly (lactic acid) nanoparticles, Journal of Biomaterials Science, Polymer Edition 25 (14-15) (2014) 1703–1716. https://doi.org/10.1080/09205063.2014.952993

[35] H. C. Barshilia, N. Gupta, Superhydrophobic polytetrafluoroethylene surfaces with leaf-like micro-protrusions through Ar + O2 plasma etching process, Vacuum 99 (2014) 42–48. https://doi.org/10.1016/j.vacuum.2013.04.020

[36] S. Rezaei, I. Manoucheri, R. Moradian, B. Pourabbas, One-step chemical vapor deposition and modification of silica nanoparticles at the lowest possible temperature and superhydrophobic surface fabrication, Chemical Engineering Journal 252 (2014) 11–16. https://doi.org/10.1016/j.cej.2014.04.100

[37] K.-J. Lu, C. Z. Liang, Y. Chen, T.-S. Chung, Unlock the secret of air blowing in developing high strength and superhydrophobic membranes for membrane distillation, Desalination 527 (2022) 115579. https://doi.org/10.1016/j.desal.2022.115579

[38] X. Wang, B. Ding, J. Yu, M. Wang, Engineering biomimetic superhydrophobic surfaces of electrospun nanomaterials, Nano Today 6 (5) (2011) 510–530. https://doi.org/10.1016/j.nantod.2011.08.004

[39] Q. Liu, H. Wang, L. Chen, W. Li, Y. Zong, Y. Sun, Z. Li, Enzymatic degradation of fluorinated poly(ε-caprolactone) (PCL) block copolymer films with improved hydrophobicity, Polymer Degradation and Stability 165 (2019) 27–34. https://doi.org/10.1016/j.polymdegradstab.2019.04.018

[40] M. Milosevic, D. B. Stojanovic, V. Simic, M. Grkovic, M. Bjelovic, P. S. Uskokovic, M. Kojic, Preparation and modeling of three-layered PCL/PLGA/PCL fibrous scaffolds for prolonged drug release, Scientific Reports 10 (1) (2020) 11126.

https://doi.org/10.1038/s41598-020-68117-9

[41] K. R. Ammann, S. F. A. Hossainy, S. Hossainy, M. J. Slepian, Hemocompatibility of polymers for use in vascular endoluminal implants, Journal of Applied Polymer Science 138 (43) (2021) 51277. https://doi.org/10.1002/app.51277

[42] E. Saracino, V. Cirillo, M. Marrese, V. Guarino, V. Benfenati, R. Zamboni, L. Ambrosio, Structural and functional properties of astrocytes on PCL based electrospun fibres, Materials Science and Engineering: C 118 (2021) 111363. https://doi.org/10.1016/j.msec.2020.111363

[43] X. Deng, M. Gould, M. A. Ali, Fabrication and characterisation of melt-extruded chitosan/keratin/PCL/PEG drug-eluting sutures designed for wound healing, Materials Science and Engineering: C 120 (2021) 111696. https://doi.org/10.1016/j.msec.2020.111696

[44] S. Park, J. Kim, M.-K. Lee, C. Park, H.-D. Jung, H.-E. Kim, T.-S. Jang, Fabrication of strong, bioactive vascular grafts with PCL/collagen and PCL/silica bilayers for small-diameter vascular applications, Materials Design 181 (2019) 108079. https://doi.org/10.1016/j.matdes.2019.108079

[45] H. Kuang, Y. Wang, Y. Shi, W. Yao, X. He, X. Liu, X. Mo, S. Lu, P. Zhang, Construction and performance evaluation of Hep/silk-PLCL composite nanofiber small-caliber artificial blood vessel graft, Biomaterials 259 (2020) 120288. https://doi.org/10.1016/j.biomaterials.2020.120288

[46] D. Liu, W. Nie, D. Li, W. Wang, L. Zheng, J. Zhang, J. Zhang, C. Peng, X. Mo, C. He, 3D printed PCL/SrHA scaffold for enhanced bone regeneration, Chemical Engineering Journal 362 (2019) 269–279. https://doi.org/10.1016/j.cej.2019.01.015

[47] A. K. Maparu, P. Singh, B. Rai, A. Sharma, S. Sivakumar, A simple,robust and scalable route to prepare sub-50 nm soft PDMS nanoparticles for intracellular delivery of anticancer drugs, Nanotechnology 33 (49) (2022) 495102. https://dx.doi.org/10.1088/1361-6528/ac8d99

[48] M. Ge, C. Cao, F. Liang, R. Liu, Y. Zhang, W. Zhang, T. Zhu, B. Yi, Y. Tang, Y. Lai, A "PDMS-in-water" emulsion enables mechanochemically robust superhydrophobic surfaces with self-healing nature, Nanoscale Horizons 5 (1) (2020) 65–73. http://dx.doi.org/10.1039/C9NH00519F

[49] S.-W. Jeong, S. Bolortuya, S. B. Eadi, S. Kim, Fabrication of superhydrophobic surfaces based on PDMS coated hydrothermal grown ZnO on PET fabrics, Journal of Adhesion Science and Technology 34 (1) (2020) 102–113. https://doi.org/10.1080/01694243.2019.1661609

[50] X. Q. Cheng, Y. Jiao, Z. Sun, X. Yang, Z. Cheng, Q. Bai, Y. Zhang, K. Wang, L. Shao, Constructing scalable superhydrophobic membranes for ultrafast water–oil separation, ACS Nano 15 (2) (2021) 3500–3508. https://doi.org/10.1021/acsnano.1c00158

[51] X. Zhang, B. Du, Y. Dai, W. Zheng, X. Ruan, G. He, Hemocompatible polydimethylsiloxane/polysulfone ultrathin composite membrane for extracorporeal membrane oxygenation, Separation and Purification Technology 302 (2022) 122028. https://doi.org/10.1016/j.seppur.2022.122028

[52] A. Park, Y. Song, E. Yi, B. T. Duy Nguyen, D. Han, E. Sohn, Y. Park, J. Jung, Y. M. Lee, Y. H. Cho, J. F. Kim, Blood oxygenation using fluoropolymer-based artificial lung membranes, ACS Biomaterials Science Engineering 6 (11) (2020) 6424–6434. https://doi.org/10.1021/acsbiomaterials.0c01251

[53] D. Dixit, C. Ghoroi, Role of randomly distributed nanoscale roughness for designing highly hydrophobic particle surface without using low surface energy coating, Journal of Colloid and Interface Science 564 (2020) 8–18. https://doi.org/10.1016/j.jcis.2019.12.041

[54] M. J. Owen, Low surface energy inorganic polymers, Comments on Inorganic Chemistry 7 (4) (1988) 195–213. https://doi.org/10.1080/02603598808072308

[55] P. Roach, D. Farrar, C. C. Perry, Interpretation of protein adsorption: surface-induced conformational changes, Journal of the AmericanChemical Society 127 (22) (2005) 8168–8173. https://doi.org/10.1021/ja042898o

[56] T. R. Roberts, M. R. S. Garren, H. Handa, A. I. Batchinsky, Toward an artificial endothelium: Development of blood-compatible surfaces for extracorporeal life support, J Trauma Acute Care Surg 89 (2S Suppl 2) (2020) S59–s68. https://doi.org/10.1097/TA.0000000000002700

[57] D. J. Weiss, Comparative Physiology of Platelets from Different Species, Springer US, Boston, MA, 1999, pp. 379–393.

[58] J. Linneweber, P. M. Dohmen, U. Kerzscher, K. Affeld, Y. Nośe, W. Konertz, The effect of surface roughness on activation of the coagulation system and platelet adhesion in rotary blood pumps, Artificial Organs 31 (5) (2007) 345–351, https://doi.org/10.1111/j.1525-1594.2007.00391.x

[59] A. A. Rownaghi, D. Bhandari, S. K. Burgess, D. S. Mikkilineni, Effects of coating solvent and thermal treatment on transport and morphological characteristics of PDMS/Torlon composite hollow fiber membrane, Journal of Applied Polymer Science 134 (42) (2017) 45418, https://doi.org/10.1002/app.45418

[60] W. Wei, S. Xia, G. Liu, X. Gu, W. Jin, N. Xu, Interfacial adhesion between polymer separation layer and ceramic support for composite membrane, AIChE Journal 56 (6) (2010) 1584–1592. https://doi.org/10.1002/aic.12086

[61] A. I. Hassan, A. L. Ahmad, Z. M. H. M. Shafie, N. D. Zaulkiflee, Fabrication of polydimethylsiloxane (PDMS) dense layer on porous polyethersulfone (PES) hollow fibre membrane with varying dip coating parameters, Journal of Physical Science 32 (1) (2021) 39–

898 56. https://doi.org/10.21315/jps2021.32.1.4
899 [62] S. M. Allen, M. Fujii, V. Stannett, H. B. Hopfenberg, J. L. Williams, The barrier properties
900 of polyacrylonitrile, Journal of Membrane Science 2 (1977) 153–163.
901 https://doi.org/10.1016/S0376-7388(00)83241-X
902 [63] B. T. Duy Nguyen, H. Y. Nguyen Thi, B. P. Nguyen Thi, D.-K. Kang, J. F.
903 Kim, The roles of membrane technology in artificial organs: Currentchallenges and
904 perspectives, Membranes 11 (4) (2021) 239. https://doi.org/10.3390/membranes11040239
905 [64] P. W. Blair, D. M. Brown, M. Jang, A. A. R. Antar, J. C. Keruly, V. S. Bachu, J. L.
906 Townsend, J. A. Tornheim, S. C. Keller, L. Sauer, D. L. Thomas, Y. C. Manabe, A. C.
907 S. Team, The clinical course of covid-19 in the outpatient setting: A prospective cohort
908 study, Open Forum Infectious Diseases 8 (2) (2021). https://doi.org/10.1093/ofid/ofab007

Highlights

Superhydrophobic polydimethylsiloxane dip-coated polycaprolactone electrospun membrane for extracorporeal membrane oxygenation

Zhuomin Jiang, Bao Tran Duy Nguyen, JeongHyeon Seo, Changgi Hong, Dongwoo Kim, Suhyun Ryu, Sohui Lee, Gyubok Lee, Young Hoon Cho*, Jeong F. Kim*, Kangwon Lee**

- Superhydrophobic membrane was designed for the ECMO membrane.
- PCL electrospun membrane was applied to the ECMO membrane substrate, and PDMS dip coating enhanced the surface hydrophobicity.
- The membrane had low protein adsorption under 10 *mg*/*m*L BSA concentrations.
- The membrane had a competitive blood oxygenation rate and hemocompatibility compared to market-dominating materials (PP and PMP).

Author statement

Superhydrophobic polydimethylsiloxane dip-coated polycaprolactone electrospun membrane for extracorporeal membrane oxygenation

Zhuomin Jiang, Bao Tran Duy Nguyen, JeongHyeon Seo, Changgi Hong, Dongwoo Kim, Suhyun Ryu, Sohui Lee, Gyubok Lee, Young Hoon Cho*, Jeong F. Kim*, Kangwon Lee**

Zhuomin Jiang: Conceptualization, Methodology, Data analysis, Writing-original draft, Writing-review & editing. **Bao Tran Duy Nguyen**: Methodology, Data analysis. **JeongHyeon Seo**: Methodology, Data analysis. **Changgi Hong**: Methodology, Data curation. **Dongwoo Kim**: Methodology, Data curation. **Suhyun Ryu**: Data curation. **Sohui Lee:** Data curation. **Gyubok Lee:** Data curation. **Young Hoon Cho:** Review & Editing, Validation, Resources. **Jeong F. Kim:** Review & Editing, Validation, Resources. **Kangwon Lee:** Supervision, Funding acquisition, Project administration.

Declaration of competing interest

Superhydrophobic polydimethylsiloxane dip-coated polycaprolactone electrospun membrane for extracorporeal membrane oxygenation

Zhuomin Jiang, Bao Tran Duy Nguyen, JeongHyeon Seo, Changgi Hong, Dongwoo Kim, Suhyun Ryu, Sohui Lee, Gyubok Lee, Young Hoon Cho*, Jeong F. Kim*, Kangwon Lee**

The authors declare no conflicts of interest.